

# Synthesis and Characterization of Nickel(II) Phosphonate Complexes Utilizing Pyridonates and Carboxylates as Co-ligands

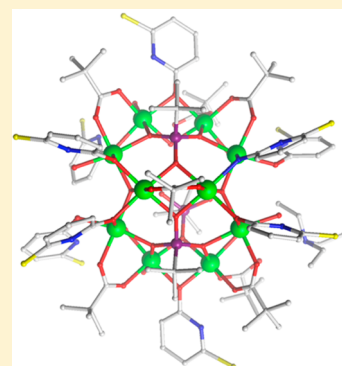
Stuart K. Langley,<sup>†</sup> Madeleine Helliwell,<sup>†</sup> Simon J. Teat,<sup>‡</sup> and Richard E. P. Winpenny<sup>\*,†,§</sup>

<sup>†</sup>School of Chemistry and <sup>§</sup>The Photon Science Institute, The University of Manchester, Oxford Road, Manchester, M13 9PL, U.K.

<sup>‡</sup>Advanced Light Source, Lawrence Berkeley Laboratory, 1 Cyclotron Road, MS2-400, Berkeley, California 94720, United States

## Supporting Information

**ABSTRACT:** The synthesis and structures of five new nickel complexes containing phosphonate ligands are reported. The compounds utilize pivalic acid (HPiv) and 6-chloro-2-pyridonate (Hchp) as co-ligands with the resulting complexes being of formulas  $[\text{Ni}_{10}(\text{chp})_4(\text{Hchp})_{4.5}(\text{O}_3\text{P}^t\text{Bu})_3(\text{Piv})_5(\text{HPiv})_2(\text{OH})_6(\text{H}_2\text{O})_{4.5}](\text{HNet}_3)\cdot 0.5\text{MeCN}\cdot 2.5\text{H}_2\text{O}$  **1**,  $[\text{Ni}_{12}(\text{chp})_{12}(\text{Hchp})_2(\text{PhPO}_3)_2(\text{Piv})_5(\text{HPiv})_2(\text{OH})_2(\text{H}_2\text{O})_6](\text{F})\cdot 4.5\text{MeCN}\cdot 2\text{H}_2\text{O}$  **2**,  $[\text{Ni}_{10}(\text{chp})_6(\text{O}_3\text{PCH}_2\text{Ph})_2(\text{Piv})_8(\text{F})_2(\text{MeCN})_4]$  **3**,  $[\text{Ni}_{10}(\text{chp})_6(\text{O}_3\text{PMe})_2(\text{Piv})_8(\text{F})_2(\text{MeCN})_4]\cdot 5\text{MeCN}\cdot 2\text{H}_2\text{O}$  **4**, and  $[\text{Ni}_{10}(\text{chp})_6(\text{O}_3\text{PCH}_2\text{Nap})_2(\text{Piv})_8(\text{F})_2(\text{MeCN})_2(\text{H}_2\text{O})_2]$  **5**. The metallic core of compounds **1** and **2** display tetra- and hexa-capped trigonal prismatic arrangements, while the metallic and phosphorus core of **3**, **4**, and **5** display three face-sharing octahedra. Variable temperature direct current (dc) magnetic susceptibility measurements reveal dominant antiferromagnetic exchange interactions within each cluster, with diamagnetic spin ground states found.



## INTRODUCTION

Paramagnetic transition metal complexes have become the focus for a great deal of research since the discovery that certain compounds behave as single molecule magnets (SMMs).<sup>1</sup> These materials display magnetic hysteresis below a blocking temperature which is a property of the molecule itself and therefore can potentially store information at unprecedented high density.<sup>2</sup> The majority of transition metal based SMMs are designed around the magnetic exchange of polynuclear complexes. Two prerequisites for SMMs are a large spin ground state ( $S$ ), with an overall cluster anisotropy (negative zero-field splitting parameter,  $D$ ). This can therefore be achieved via the arrangement of paramagnetic ions in a cluster array, often guided by the selection of the bridging ligands and of the transition metal, leading to favorable magnetic exchange interactions and total cluster anisotropy.

With this in mind transition metal phosphonate complexes have been studied in depth recently because of the discovery that discrete multinuclear clusters can be stabilized, overcoming the restrictions of solubility which previously hampered efforts in this area.<sup>3</sup> Stable layered 1-D and 2-D coordination polymers are commonly isolated as the insoluble product;<sup>4</sup> however, preventing the formation of these extended lattices has allowed us to develop key synthetic strategies toward the isolation of magnetically interesting 0-D molecular cluster complexes. To prevent the formation of these extended structures, several general methods are now employed toward the synthesis of molecular metal phosphonates. Two of these methods involves use of a co-ligand alongside the phosphonate. In one of these routes, referred to as the cluster expansion method, the phosphonic acid is reacted with a preformed polymeric complex that already contains co-ligands, resulting in larger

polymetallic compounds. The phosphonate displaces some of these ancillary ligands, which would in turn bridge to further metals, hence forming a larger product, usually related to the starting preformed complex.<sup>5</sup> The second synthetic strategy utilized simple metal salts with addition of a co-ligand such as Hchp (2-chloro-6-hydroxypyridine) in a certain mole ratio. The co-ligands restrict oligomerization by occupying some of the metal coordination sites and hence enhance the solubility of the resultant metal phosphonate cages, enabling us to isolate many novel and varied metal topologies.<sup>6</sup> In addition to these methods a strategy which involves using very bulky phosphonate ligands has also proved fruitful in isolating several small 3d molecular complexes.<sup>7</sup> Solvothermal techniques are also providing a route to molecular phosphonate complexes.<sup>8</sup> Utilizing these methods a large number of vanadium,<sup>9</sup> manganese,<sup>10</sup> iron<sup>5,11</sup> and cobalt<sup>6,12</sup> clusters has now been synthesized. There is also a growing body of work on 3d–4f<sup>13</sup> and 4f-phosphonates.<sup>14</sup>

There are many fewer nickel based phosphonate complexes, with only three examples found in the literature:  $[\text{Ni}^{\text{II}}_8(\text{OH})_4(\text{OH}_2)_2(\text{O}_3\text{PCH}_2\text{Ph})_2(\text{O}_2\text{C}^t\text{Bu})_8(\text{HO}_2\text{C}^t\text{Bu})_6]$ ,  $[\text{Ni}^{\text{II}}_9(\text{OH})_3(\text{OH}_2)_3(\text{O}_3\text{PCH}_2\text{Ph})(\text{HO}_3\text{PCH}_2\text{Ph})(\text{O}_2\text{C}^t\text{Bu})_8(\text{chp})_4(\text{HO}_2\text{C}^t\text{Bu})_2(\text{OH}_2)]$  (chp = 6-chloro-2-hydroxypyridonate) and  $[\text{Ni}^{\text{II}}_{12}(\text{OH})_4(\text{O}_3\text{PPh})_4(\text{O}_2\text{C}^t\text{Bu})_{12}(\text{L})_6]$  (where L is a disordered mixture of  $\text{HO}_2\text{CMe}$ ,  $\text{MeCN}$ ,  $\text{H}_2\text{O}$  and or  $\text{HO}_2\text{C}^t\text{Bu}$ ).<sup>15</sup> The co-ligands found to isolate these complexes involve carboxylate and/or pyridonate ligands, which have been used to isolate a plethora of cobalt based phosphonate compounds.<sup>6</sup> Initial attempts toward the isolation

Received: October 24, 2013

Published: January 6, 2014

Table 1. Crystal Data and Refinement Parameters for Compounds 1–5

	1	2	3	4	5
formula <sup>a</sup>	Ni <sub>10</sub> C <sub>96.5</sub> H <sub>159.5</sub> Cl <sub>8.5</sub> N <sub>10</sub> O <sub>44.5</sub> P <sub>3</sub>	Ni <sub>12</sub> C <sub>126</sub> H <sub>130.5</sub> Cl <sub>14</sub> N <sub>18.5</sub> O <sub>44</sub> P <sub>2</sub>	Ni <sub>10</sub> C <sub>92</sub> H <sub>116</sub> Cl <sub>6</sub> F <sub>2</sub> N <sub>10</sub> O <sub>28</sub> P <sub>2</sub>	Ni <sub>10</sub> C <sub>90</sub> H <sub>123</sub> Cl <sub>6</sub> F <sub>2</sub> N <sub>15</sub> O <sub>30</sub> P <sub>2</sub>	Ni <sub>10</sub> C <sub>96</sub> H <sub>118</sub> Cl <sub>6</sub> F <sub>2</sub> N <sub>10</sub> O <sub>30</sub> P <sub>2</sub>
<i>M<sub>r</sub></i>	3152.99	3909.88	2709.69	2794.77	2763.69
crystal system	triclinic	triclinic	monoclinic	triclinic	monoclinic
space group	<i>P</i> $\bar{1}$	<i>P</i> $\bar{1}$	<i>P</i> <sub>2</sub> / <i>n</i>	<i>P</i> $\bar{1}$	<i>C</i> 2/ <i>c</i>
<i>a</i> [Å]	19.0975(10)	18.9182(14)	14.9120(7)	12.7616(8)	20.352(6)
<i>b</i> [Å]	19.4713(10)	19.0078(14)	23.1537(12)	13.9766(9)	20.639(6)
<i>c</i> [Å]	23.0256(12)	26.781(2)	16.1217(8)	18.4661(11)	27.040(7)
$\alpha$ [deg]	71.9180(10)	102.0500(10)	90	92.7450(10)	90
$\beta$ [deg]	82.6050(10)	92.277(2)	90.734(2)	104.2800(10)	90.028(4)
$\gamma$ [deg]	76.8900(10)	103.3590(10)	90	107.8710(10)	90
<i>V</i> [Å <sup>3</sup> ]	7911.4(7)	9123.9(12)	5565.8(5)	3010.5(3)	11358(5)
<i>T</i> [K]	100(2)	100(2)	150(2)	100(2)	100(2)
<i>Z</i>	2	2	2	1	4
crystal size [mm]	0.60 × 0.40 × 0.20	0.6 × 0.6 × 0.2	0.10 × 0.08 × 0.01	0.6 × 0.6 × 0.2	0.4 × 0.4 × 0.2
$\rho_{\text{calcd}}$ [g cm <sup>-3</sup> ]	1.314	1.422	1.617	1.542	1.614
crystal shape and color	plate green	block green	plate green	block green	plate green
radiation	Mo <sub>K<math>\alpha</math></sub>	Mo <sub>K<math>\alpha</math></sub>	synchrotron	Mo <sub>K<math>\alpha</math></sub>	Mo <sub>K<math>\alpha</math></sub>
ind.reflns	63527	53058	64081	17388	32094
<i>R</i> <sub>int</sub>	0.0481	0.0228	0.0438	0.0127	0.1311
reflns with <i>I</i> > 2 $\sigma$ ( <i>I</i> )	18296	23640	12979	10897	7029
parameters	1727	2154	721	739	710
restraints	166	87	18	20	43
<i>R</i> <sub>1</sub> (obs), <i>wR</i> <sub>2</sub> (obs) <sup>b</sup>	0.0864, 0.2606	0.0611, 0.1825	0.0428, 0.1144	0.0280, 0.0774	0.0677, 0.1457
goodness of fit	1.041	1.030	1.044	1.007	0.954
largest residuals [e Å <sup>-3</sup> ]	1.780, -1.388	1.568, -1.107	1.417, -0.732	1.232, -0.446	1.407, -1.473

<sup>a</sup>Including solvate molecules. <sup>b</sup> $R_1 = \sum ||F_o| - |F_c|| / \sum |F_o|$ ,  $wR_2 = \{ \sum [w(F_o^2 - F_c^2)^2] / \sum [w(F_o^2)^2] \}^{1/2}$ .

of Ni<sup>II</sup> clusters via the adaptation of the Co<sup>II</sup> methodology, using the co-ligand 2-chloro-6-hydroxypyridine, did not yield any positive results.<sup>6a–d</sup> Recently however we have discovered a number of Co<sup>II</sup> phosphonate cages that contain two co-ligands, -Hchp (2-chloro-6-hydroxypyridine) and carboxylic acids, similar to the nonanuclear complex above.<sup>6e</sup> Adapting this synthetic method we are able to report the synthesis, X-ray analysis, and magnetic characterization of five new Ni<sup>II</sup> phosphonate clusters.

## EXPERIMENTAL SECTION

**Preparation of Compounds.** All reagents, metal salts, and ligands were used as obtained from Aldrich. Analytical data, listed, were obtained by the microanalytical service of the University of Manchester.

**Synthesis of (HNEt<sub>3</sub>)[Ni<sub>10</sub>(chp)<sub>4</sub>(Hchp)<sub>4.5</sub>(O<sub>3</sub>P<sup>i</sup>Bu)<sub>3</sub>(Piv)<sub>5</sub>(HPiv)<sub>2</sub>(OH)<sub>6</sub>(H<sub>2</sub>O)<sub>4.5</sub>]-0.5MeCN-2.5H<sub>2</sub>O 1.** Nickel tetrafluoroborate hexahydrate (0.63 mL, 2 mmol) was dissolved in acetonitrile (25 mL). To this solution 6-chloro-2-hydroxypyridine (0.52 g, 4 mmol), <sup>t</sup>BuPO<sub>3</sub>H<sub>2</sub> (0.046 g, 0.33 mmol), pivalic acid (0.20 g, 2 mmol), and triethylamine (0.79 mL, 5.66 mmol) were sequentially added, resulting in a green solution, which was stirred for 6 h. After this time the solution was allowed to slowly evaporate, with green crystals of **1** appearing after 1 week. Yield 0.07 g, 11.5%. Elemental analysis (%) calculated for Ni<sub>10</sub>C<sub>92</sub>H<sub>139</sub>N<sub>9</sub>O<sub>42</sub>P<sub>3</sub>Cl<sub>9</sub>: C 36.32, H 4.61, N 4.14; found C 37.12, H 4.34, N 4.00.

**Synthesis of [Ni<sub>12</sub>(chp)<sub>12</sub>(Hchp)<sub>2</sub>(PhPO<sub>3</sub>)<sub>2</sub>(Piv)<sub>5</sub>(HPiv)<sub>2</sub>(OH)<sub>2</sub>(H<sub>2</sub>O)<sub>6</sub>]-0.5MeCN-2H<sub>2</sub>O 2.** Reaction as **1** except PhPO<sub>3</sub>H<sub>2</sub> (0.052 g, 0.33 mmol) was used in place of <sup>t</sup>BuPO<sub>3</sub>H<sub>2</sub>. Yield 0.12 g, 19.4%. Elemental analysis (%) calculated for Ni<sub>12</sub>C<sub>117</sub>H<sub>133</sub>N<sub>14</sub>O<sub>42</sub>P<sub>2</sub>Cl<sub>15</sub>: C 37.93, H 3.62, N 5.29; found C 37.56, H 3.45, N 5.23.

**Synthesis of [Ni<sub>10</sub>(chp)<sub>6</sub>(O<sub>3</sub>PCH<sub>2</sub>Ph)<sub>2</sub>(Piv)<sub>8</sub>(F<sub>2</sub>(MeCN)<sub>4</sub>)] 3.** Reaction as **1** except PhCH<sub>2</sub>PO<sub>3</sub>H<sub>2</sub> (0.058 g, 0.33 mmol) was used in place of <sup>t</sup>BuPO<sub>3</sub>H<sub>2</sub>. Yield 0.06 g, 11.0%. Elemental analysis (%) calculated for Ni<sub>10</sub>C<sub>92</sub>H<sub>116</sub>N<sub>10</sub>O<sub>28</sub>P<sub>2</sub>Cl<sub>6</sub>F<sub>2</sub>: C 40.78, H 4.32, N 5.17; found C 40.98, H 4.67, N 5.45.

**Synthesis of [Ni<sub>10</sub>(chp)<sub>6</sub>(O<sub>3</sub>PMe)<sub>2</sub>(Piv)<sub>8</sub>(F<sub>2</sub>(MeCN)<sub>4</sub>)]-5MeCN-2H<sub>2</sub>O 4.** Reaction as **1** except MePO<sub>3</sub>H<sub>2</sub> (0.033 g, 0.33 mmol) was used in place of <sup>t</sup>BuPO<sub>3</sub>H<sub>2</sub>. Yield 0.05 g, 10.0%. Elemental analysis (%) calculated for Ni<sub>10</sub>C<sub>80</sub>H<sub>108</sub>N<sub>10</sub>O<sub>28</sub>P<sub>2</sub>Cl<sub>6</sub>F<sub>2</sub>: C 37.57, H 4.26, N 5.48; found C 36.23, H 4.01, N 5.12.

**Synthesis of [Ni<sub>10</sub>(chp)<sub>6</sub>(O<sub>3</sub>PCH<sub>2</sub>Nap)<sub>2</sub>(Piv)<sub>8</sub>(F<sub>2</sub>(MeCN)<sub>4</sub>)] 5.** Reaction as **1** except NapCH<sub>2</sub>PO<sub>3</sub>H<sub>2</sub> (0.074 g, 0.33 mmol) was used in place of <sup>t</sup>BuPO<sub>3</sub>H<sub>2</sub> and recrystallization was from MeCN/Et<sub>2</sub>O. Yield 0.07 g, 12.4%. Elemental analysis (%) calculated for Ni<sub>10</sub>C<sub>100</sub>H<sub>120</sub>N<sub>10</sub>O<sub>28</sub>P<sub>2</sub>Cl<sub>6</sub>F<sub>2</sub>: C 42.75, H 4.30, N 4.99; found C 42.68, H 4.23, N 4.91.

**Structure Determinations.** X-ray crystallographic measurements for compounds **1**, **2**, **4**, and **5** were collected on a Bruker SMART CCD diffractometer (Mo-*K $\alpha$* ,  $\lambda = 0.71073$  Å). Data for compound **3** was collected on a Bruker AXS SMART CCD area detector attached to station 9.8 at the CCLRC Daresbury synchrotron radiation source ( $\lambda = 0.6932$  Å). In all cases the selected crystals were mounted on the tip of a glass pin using Paratone-N oil and placed in the cold flow (100 K) produced with an Oxford Cryocooling device.<sup>16</sup> Integrated intensities were obtained with SAINT+,<sup>13</sup> and they were corrected for absorption using SADABS.<sup>17</sup> The structures were all solved by direct methods and refined by full matrix least-squares on all *F*<sup>2</sup> data.<sup>17</sup> Full crystallographic details can be found in CIF format: CCDC for **1**–**5** 968474–968478. Crystal data and refinement parameters are given in Table 1. Selected bond length ranges for the five compounds are given in Supporting Information, Tables S1–S5.

**Magnetic Measurements.** The magnetic properties of polycrystalline samples of **1**–**5** were investigated using a Cryogenic M600 SQUID magnetometer. Data have been corrected for the diamagnet-

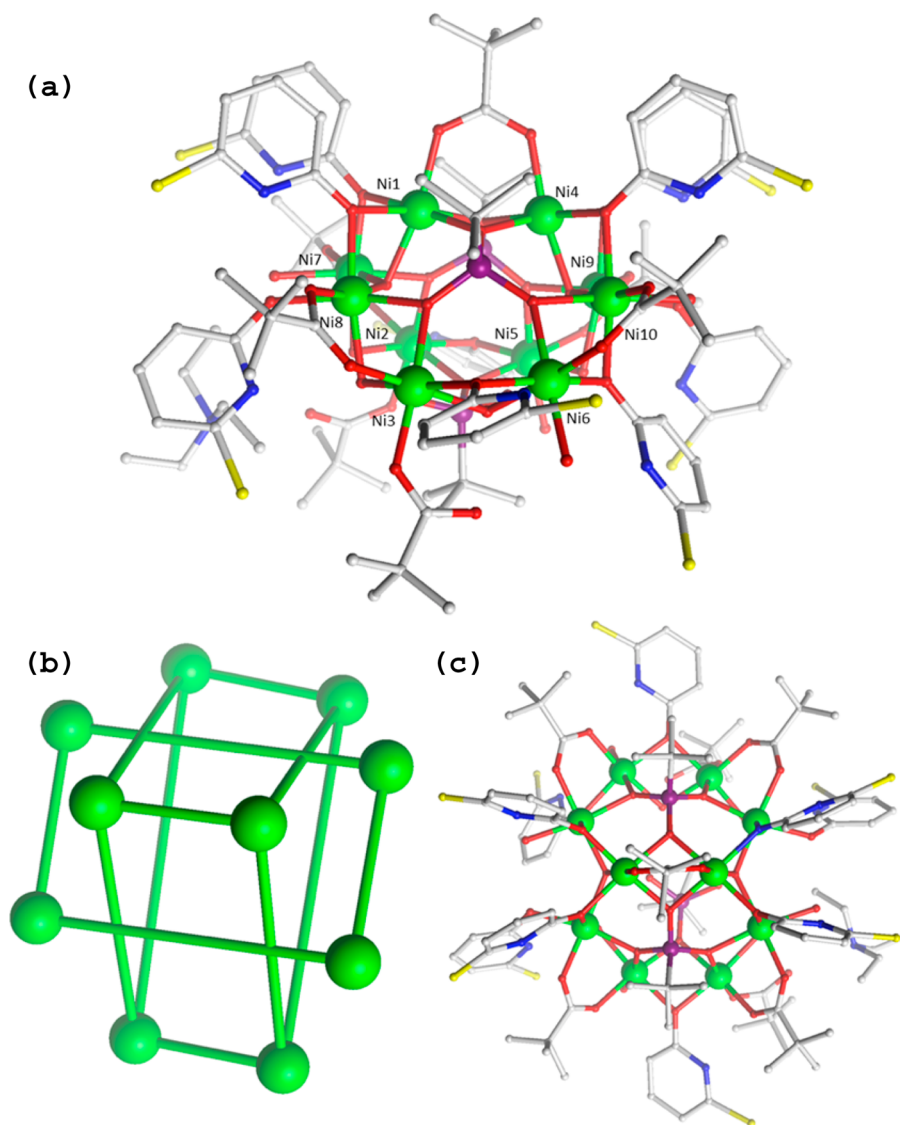


**Figure 1.** (a) Molecular structure of **1**, side view; (b) the metal core showing a rectangle lying within a trigonal prism; (c) top down view displaying the two fused hexanuclear rings. Solvent, disordered, and H-atoms are omitted for clarity. Color scheme: Ni, green; P, magenta; N, blue; O, red; C, light gray; Cl, yellow.

ism of the sample holder and diamagnetic corrections based on Pascal's constants have been used in the calculations.

## RESULTS AND DISCUSSION

**Structural Analysis.** All complexes follow a general synthetic procedure of reacting a Ni<sup>II</sup> salt in MeCN, with Hchp, pivalic acid, RPO<sub>3</sub>H<sub>2</sub>, and NEt<sub>3</sub>. By variation of the organic R group of the phosphate we are able to access five new structures. When *tert*-butylphosphonic acid is used crystals of (HNEt<sub>3</sub>)[Ni<sub>10</sub>(chp)<sub>4</sub>(Hchp)<sub>4.5</sub>(O<sub>3</sub>P<sup>t</sup>Bu)<sub>3</sub>(Piv)<sub>5</sub>(HPiv)<sub>2</sub>(OH)<sub>6</sub>(H<sub>2</sub>O)<sub>4.5</sub>]·0.5MeCN·2.5H<sub>2</sub>O **1** can be grown. Compound **1** crystallizes in the triclinic space group *P* $\bar{1}$ , with the asymmetric unit containing the entire cluster as well as MeCN and H<sub>2</sub>O solvent molecules.

It was found from the X-ray analysis that compound **1** is a decanuclear Ni<sup>II</sup> complex (Figure 1a). The metallic core arrangement of **1** shows that six of the ions, Ni1–Ni6, lie on the vertices of a trigonal prism, with Ni7 and Ni8 capping the edges of one triangular face, with Ni9 and Ni10 capping the opposite face. This results in a rectangle lying within the prism

(Figure 1b). Of the three phosphonate ligands present, two adopt the 6.222 [Harris notation<sup>18</sup>] bonding mode, with Ni1 and Ni4 being bonded by both (Figure 1c). It is found that each phosphonate ligand lies on two of the rectangular faces of the prism. The third phosphonate displays the 2.200 bonding mode bridging Ni3 to Ni6 across a rectangular face of the prism, with the noncoordinating O-atoms accepting H-bonds from hydroxide ligands in the complex. Trigonal prismatic based clusters have been found to be a common structural motif when utilizing the ligand Hchp;<sup>17</sup> however such a metallic arrangement as **1** is new.

A second perspective of the decanuclear core reveals a similar arrangement to which has previously been observed for several recent cobalt-phosphonate based clusters. That particular motif describes a near planar hexagonal ring with a 6.222 phosphonate lying at its center.<sup>6d,e</sup> Compound **1** displays two such fused rings with Ni1 and Ni4 being common to both (Figure 1c). The metal ions in addition to the phosphonate ligands are stabilized by pyridonate, carboxylate, and hydroxide bridging ligands. Six hydroxide ions are found within **1**, four are

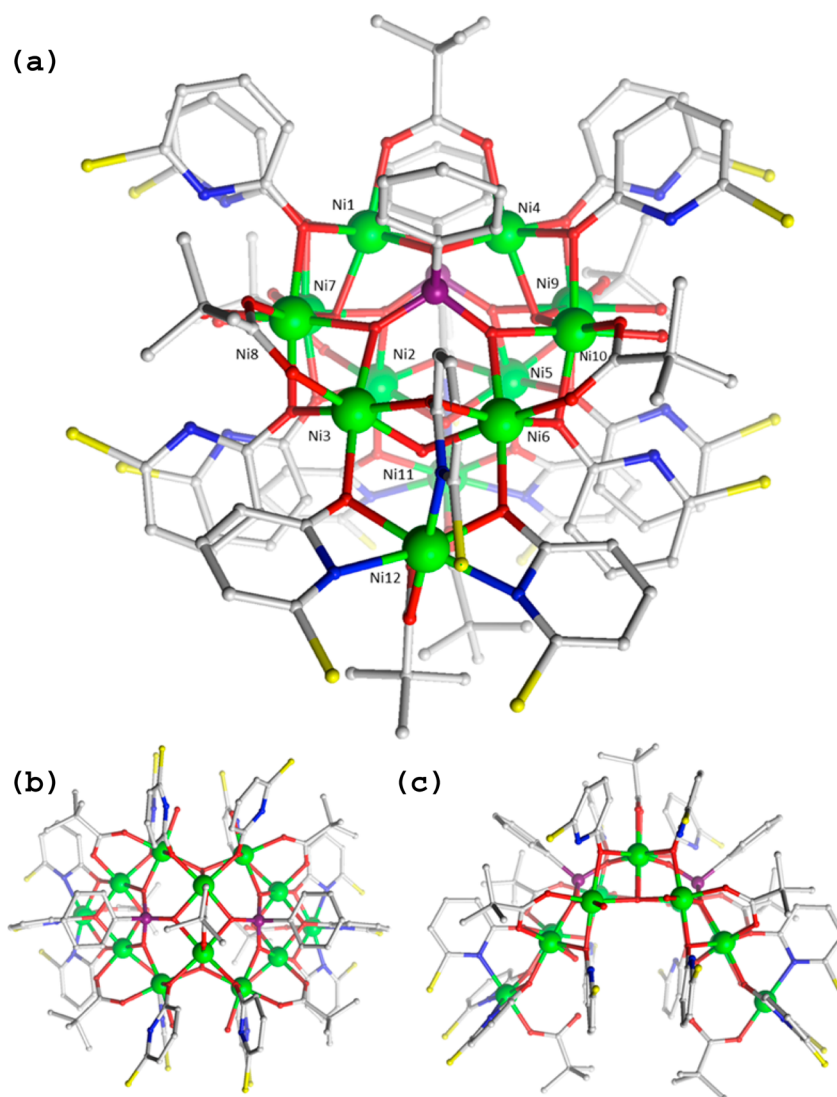


**Figure 2.** (a) Molecular structure of **2**, side view; (b) top down view highlighting the two fused hexanuclear rings; (c) end on view, highlighting the cavity. Solvent, disordered, and H-atoms are omitted for clarity. Color scheme used is the same as with Figure 1.

$\mu_2$  and two are  $\mu_3$  bridging (binding to Ni1, Ni7, and Ni10, and Ni4, Ni9, and Ni10, respectively, Figure 1a). Of the six, five bridge the prism to the capping sites, while a single hydroxide bridges across a rectangular edge of the prism. There are four  $\text{chp}^-$  ligands, with four fully occupied and one-half occupied Hchp ligands present. The four  $\text{chp}^-$  ligands all display the 2.20 bonding mode. The Hchp ligands are found to be protonated via the N-atom, with three of the ligands also displaying the 2.20 bonding mode, while the final fully and the half occupied ligand, lie terminal, with the 1.10 bonding mode. There are five 2.11 pivalates, four of them bridge the prism to the caps, while the fifth lies at the apex of the structure bridging Ni1 and Ni4. Two 1.10 pivalic acid ligands are found to lie terminal, coordinating to Ni2 and Ni3. While it is difficult to unambiguously determine the position of the H-atoms from X-ray crystallographic data alone, H-bonding distances between the various N- and O-donor atoms were used to rationalize the protonation levels of the ligands present (Supporting Information, Figure S1). Finally there are four fully occupied water molecules that all coordinate terminally, two are bound to Ni5 and Ni6 of the prism, with the final two bound to the capping sites Ni8 and Ni9. A half occupied water molecule is

also found to be coordinated to Ni10 when the half occupied Hchp ligand is absent. Compound **1** is therefore exclusively bonded via oxygen donor atom donors. The nickel sites are all six coordinate with distorted octahedral geometries, with an average Ni<sup>II</sup>–O bond length of 2.06 Å. A protonated triethylamine ( $\text{HNEt}_3$ ) cation is also present and forms a {N–H $\cdots$ O} H-bond to a terminal pivalic acid ligand. There are no significant intramolecular interactions (Supporting Information, Figures S2 and S3).

By changing the phosphonate from *tert*-butylphosphonic acid to phenylphosphonic acid we were able to isolate a related cluster. The resulting complex,  $[\text{Ni}_{12}(\text{chp})_{12}(\text{Hchp})_2(\text{PhPO}_3)_2(\text{Piv})_5(\text{HPiv})_2(\text{OH})_2(\text{H}_2\text{O})_6](\text{F})\cdot 4.5\text{MeCN}\cdot 2\text{H}_2\text{O}$  (**2**) (Figure 2) is a dodecanuclear Ni<sup>II</sup> cage, which crystallizes in the triclinic space group  $P\bar{1}$ .

X-ray analysis reveals that the asymmetric unit contains the entire cluster with a fluoride counterion and solvent MeCN and water molecules. Compound **2** is closely related to that of **1**, with an identical decanuclear fragment found, [Ni1–Ni10], with the addition of two further nickel ions, [Ni11 and Ni12], and, as a consequence, a modified ligand backbone. A trigonal prism is therefore observed with Ni1–Ni6, lying at its vertices,

with Ni7 and Ni8 capping the edges of one triangular face, with Ni9 and Ni10 capping the opposite face. The additional Ni<sup>II</sup> sites, Ni11 and Ni12, “cap” below the edge of the bottom rectangular face. This overall leads to the presence of a cavity or channel in the structure (Figure 2c). The two phosphonate ligands adopt the 6.222 mode, bonding to ten of the nickel sites, with Ni1 and Ni4 being bonded by both. These ligands again lie on two of the rectangular faces of the prism, identical to **1**, resulting in the same hexagonal ring motif as observed for previous phosphonate clusters (Figure 2b).<sup>6d,e</sup> There are 12 chp<sup>−</sup> ligands present, 6 adopt the 2.20 bonding mode, 2 the 3.21, and 4 the 2.21 modes. Two protonated Hchp ligands are also found, which are protonated via the N-atom, adopting the 2.20 bonding mode. The two Hchp and two of the 2.20 chp<sup>−</sup> ligands bridge from Ni1 and Ni4 to the nickel capping sites, [Ni7–Ni10]. The remaining four 2.20 chp<sup>−</sup> ligands each bridge from [Ni2, Ni3, Ni5, and Ni6] to four of the metal caps, [Ni7–Ni10]. Ni11 is bonded to the Ni<sup>II</sup> sites of the bottom rectangular face of the prism via a single 3.21 and two 2.21 chp<sup>−</sup> ligands; this is also the case for Ni12 on the opposite side of the cluster. There are two  $\mu_3$  hydroxides present which bond [Ni1 to Ni7 and Ni8] and [Ni4 to Ni9 and Ni10] identical to **1**. Two  $\mu_2$  water molecules are found to bridge [Ni2 to Ni5] and [Ni3 and Ni6] of the bottom rectangular face.

There are five 2.11 pivalates, four of them bridge the prism to the triangular face capping sites, while the fifth lies at the apex of the structure bridging Ni1 and Ni4, again identical to **1**. Two pivalic acid ligands lie terminal adopting the 1.10 mode, coordinating to Ni11 and Ni12. There are four terminal water molecules found bonding to Ni7, Ni8, Ni9, and Ni10. The nickel sites are all six coordinate with octahedral geometries, with average Ni–O and Ni–N bond lengths of 2.05 and 2.15 Å, respectively. It is found that a water molecule and a disordered fluoride ion are located in the cavity of the complex. There are numerous intramolecular hydrogen bonding interactions for compound **2**. While it is difficult to determine the position of the H-atoms from X-ray crystallographic data alone, as with **1**, H-bonding distances which are present between the various N- and O-donor atoms were used to rationalize the protonation levels of the ligands present (Supporting Information, Figure S4). The two Hchp ligands that are protonated via the N-atom form a H-bond to a neighboring pivalate O-atom. The four terminal water molecules exhibit two different H-bonding modes. Two water molecules form H-bonds to N-atoms of a chp<sup>−</sup> ligand and to a neighboring water molecule, while two form H-bonds to the N-atoms of two chp<sup>−</sup> ligands. The two  $\mu_3$  hydroxide ligands form H-bonds with the water molecule found in the cavity of the molecule, as do one of the H-atoms of both of the bridging water ligands. The second H-atom is found to H-bond to a O-atom of the terminal pivalic acid ligand, while the H-atom of the two pivalic acid ligands are found to H-bond to the disordered F<sup>−</sup> ions. There are no significant intramolecular interactions (Supporting Information, Figure S5).

Upon further variation of the phosphonate ligand in which we utilized benzyl-, methyl-, and naphthylmethyl-phosphonic acids, we were able to isolate three analogous cages. The resulting complexes are of formulas [Ni<sub>10</sub>(chp)<sub>6</sub>(O<sub>3</sub>PCH<sub>2</sub>Ph)<sub>2</sub>(Piv)<sub>8</sub>(F)<sub>2</sub>(MeCN)<sub>4</sub>] **3**, [Ni<sub>10</sub>(chp)<sub>6</sub>(O<sub>3</sub>PMe)<sub>2</sub>(Piv)<sub>8</sub>(F)<sub>2</sub>(MeCN)<sub>4</sub>]·5MeCN·2H<sub>2</sub>O **4**, and [Ni<sub>10</sub>(chp)<sub>6</sub>(O<sub>3</sub>PCH<sub>2</sub>Nap)<sub>2</sub>(Piv)<sub>8</sub>(F)<sub>2</sub>(MeCN)<sub>2</sub>(H<sub>2</sub>O)<sub>2</sub>] **5**. Compound **3** (Figure 3) crystallizes in the monoclinic space group *P2<sub>1</sub>/n*, **4** crystallizes in the triclinic space group *P1̄*, and **5** crystallizes in the monoclinic space group *C2/c*, with the asymmetric unit for

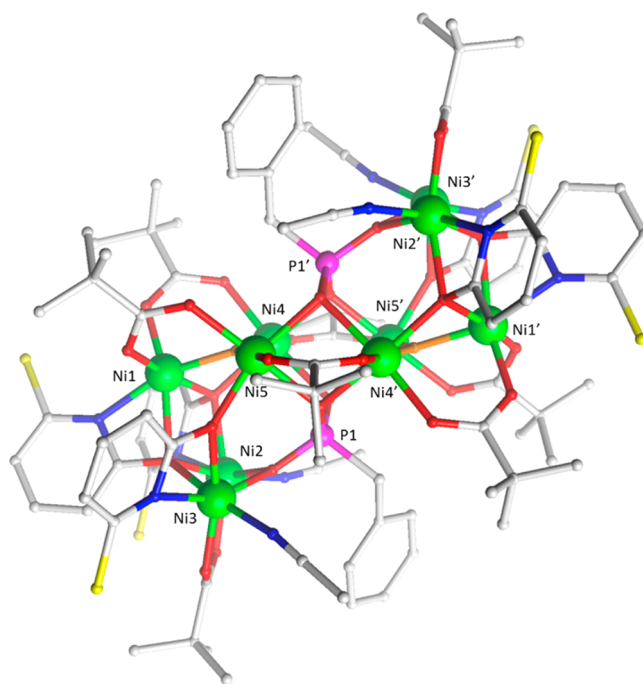


**Figure 3.** Molecular structure of **3**. Disordered and H-atoms are omitted for clarity. The color scheme used is the same as with Figure 1, with F, orange.

each consisting of half the cluster and all lie about an inversion center.

Compounds **3**, **4**, and **5** are all decanuclear Ni<sup>II</sup> cages. The metal topology and the ligand backbone presented in this study are analogous to previously reported cobalt-phosphonate-chp-carboxylate clusters.<sup>6e</sup> Each complex reveals five nickel ions, Ni1–Ni5, and a phosphorus atom, P1, in the asymmetric unit, forming a distorted octahedral arrangement. Because of the inversion symmetry, two further octahedra are formed, resulting in three face sharing octahedra. The second “central” octahedral unit consists of four nickel ions, Ni4, Ni5, Ni4', and Ni5', which lie in the equatorial positions, and two phosphorus atoms, P1 and P1', lying axially. The third octahedron, is the symmetry equivalent (s.e.) of the first. The complex is held together primarily by two 6.222 phosphonates and two  $\mu_3$  fluoride ions. The phosphonate ligands coordinate to all of the nickel ions except for Ni1 and Ni1', while the  $\mu_3$  fluoride ions bridge Ni1 to Ni4 and Ni5 (and the s.e. sites). The assignment of the fluoride bridges were unambiguously confirmed (versus hydroxide) for the equivalent {Co<sub>10</sub>} complexes and found to also be present in the case of **3–5**. The complexes are stabilized around the periphery of the cage by pyridonate (chp<sup>−</sup>) and pivalate ligands. There are six bridging chp<sup>−</sup> ligands, four display the 3.31 mode, each bonding to [Ni1, Ni2, and Ni3], [Ni1, Ni2, and Ni4], and to the s.e. ions, while two adopt the 2.21 mode binding Ni3 to Ni5 and the s.e.'s respectively. Eight 2.11 pivalate ligands are present, six of which bridge across the edges of the two outer octahedra, while the final two bridge across an edge of the central {Co<sub>4</sub>P<sub>2</sub>} octahedral unit. There are four terminal MeCN molecules found for **3** and **4**, completing the coordination spheres for Ni2 and Ni3 and s.e. sites, while two MeCN and two H<sub>2</sub>O molecules are found for compound **5**. All ten nickel sites are six coordinate with distorted octahedral geometries, with average Ni–O, Ni–F, and Ni–N bond lengths of 2.07, 2.01, and 2.09 Å for **3** respectively. Packing diagrams of

structures 3–5 are given as Supporting Information, Figures S6–S8; the only possible intramolecular interaction is an edge-to-face aromatic- $\pi$ ...C–H bond in 5 (Supporting Information, Figure S8).

**Magnetic Data.** Direct current (dc) magnetic susceptibility measurements were performed on polycrystalline samples of 1, 2, and 5 in the temperature range 2–300 K, in a magnetic field of 0.1 T, with compound 5 being representative of the face sharing octahedral metallic core topology. The  $\chi_M T$  ( $\chi_M$  = molar magnetic susceptibility) versus  $T$  plots for 1, 2, and 5 are shown in Figure 4. The decanuclear complexes, 1 and 5 display

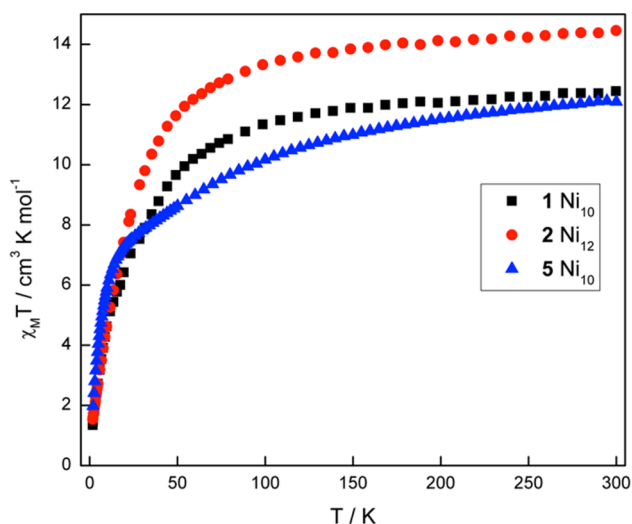


**Figure 4.**  $\chi_M T$  versus  $T$  plots of compounds 1, 2, and 5, with an applied dc magnetic field of 0.1 T.

room temperature  $\chi_M T$  values of 12.46 and 12.11  $\text{cm}^3 \text{K mol}^{-1}$ , respectively, while the dodecanuclear compound, 2, reveals a  $\chi_M T$  room temperature value of 14.56  $\text{cm}^3 \text{K mol}^{-1}$ . These values are consistent with 10 and 12 uncoupled  $\text{Ni}^{\text{II}}$  centers ( $S = 1$ ) with  $g$  values slightly greater than 2, as expected for octahedral  $\text{Ni}^{\text{II}}$  ions. The  $\chi_M T$  products for 1 and 2 decrease gradually upon lowering the temperature, before a rapid drop below  $\sim 60$  K, reaching 1.348  $\text{cm}^3 \text{K mol}^{-1}$  for 1 and 1.57  $\text{cm}^3 \text{K mol}^{-1}$  for 2 at 2 K. For 5 the  $\chi_M T$  value decreases more rapidly as the temperature is reduced down to 20 K, below which a sharp decrease occurs reaching 2.02  $\text{cm}^3 \text{K mol}^{-1}$  at 2 K. This behavior shows that the magnetic exchange in all three cases is dominated by antiferromagnetic interactions, and the ground states are most likely diamagnetic. Because of the large size and complexity of the clusters, however, fitting of the experimental magnetic data could not be performed to determine the pairwise exchange interactions. No further measurements to explore for SMM behavior were deemed necessary because of the diamagnetic spin ground states for each cluster. Plots of  $1/\chi$  against  $T$  are linear from 60–300 K (Supporting Information, Figures S9–S11); fitting this linear region allows us to calculate Weiss constants: for 1,  $-16.5$  K; for 2,  $-14.8$  K; for 5,  $-23.6$  K. These Weiss constants are consistent with antiferromagnetic exchange interactions.

## CONCLUSIONS

In summary we have synthesized and characterized five novel nickel phosphonate cages via the inclusion of two co-ligands, 6-chloro-2-hydroxypyridine and pivalic acid, with the final

products being controlled by variation of the organic R group of the phosphonate ligand. The complexes fall into two distinct families, compounds 1 and 2 display tetra- and hexa-capped trigonal prismatic based metallic core topologies, while 3, 4, and 5 display face sharing octahedral motifs. For compounds 3, 4, and 5 it is found that this arrangement is isostructural to the  $\text{Co}^{\text{II}}$  analogues.<sup>6c</sup> Compounds 1 and 2 display a motif similar to that of a cobalt/chp/phosphonate compound of formula  $[\text{HNEt}_3][\text{Co}_8(\text{chp})_{10}(\text{Hchp})_2(\text{O}_3\text{PPh})_2(\text{NO}_3)_3]$ .<sup>6b</sup> This complex displays a tetra capped trigonal prismatic motif with two phosphorus atoms found at two vertices of the prism. In the case of 1 and 2 the phosphorus atoms lie at the center of opposite rectangular faces. Compounds 1–5 are rare examples of nickel phosphonate complexes indicating that phosphonate cluster chemistry which is extremely well developed for manganese,<sup>10</sup> iron<sup>5,11</sup> and cobalt<sup>6,12</sup> can be extended to nickel. The magnetic susceptibility data for all complexes display dominant antiferromagnetic exchange interactions resulting in small or zero ground spin states; we hope, however, that we can adapt this reaction scheme via variation of the phosphonate or co-ligands to assemble further cages with the hope of producing more magnetically interesting compounds.

## ASSOCIATED CONTENT

### Supporting Information

Crystallographic data in CIF format (CCDC 968474–968478). Further details are given in tables of bond lengths, figures showing the packing of molecules in the crystal, and Curie–Weiss plots of magnetic data. This material is available free of charge via the Internet at <http://pubs.acs.org>.

## AUTHOR INFORMATION

### Corresponding Author

\*E-mail: [richard.winpenny@man.ac.uk](mailto:richard.winpenny@man.ac.uk).

### Notes

The authors declare no competing financial interest.

## ACKNOWLEDGMENTS

We thank the EPSRC(U.K.) for funding for a studentship (S.L.). We are also grateful to the EC-TMR “QueMolNa” for support. R.E.P.W. is grateful to The Royal Society for a Wolfson Merit Award. The ALS is supported by the Director, Office of Science, Office of Basic Energy Sciences, of the U.S. Department of Energy under contract no. DE-AC02-05CH11231.

## REFERENCES

- (1) (a) Sessoli, R.; Gatteschi, D.; Caneschi, A.; Novak, M. A. *Nature* **1993**, *365*, 141. (b) Christou, G.; Gatteschi, D.; Hendrickson, D. N.; Sessoli, R. *M. R. S. Bull.* **2000**, *25*, 66.
- (2) (a) Leuenberger, M. N.; Loss, D. *Nature* **2001**, *410*, 789. (b) Mannini, M.; Pineider, F.; Sainctavit, P.; Danieli, C.; Otero, E.; Sciancalepore, C.; Talarico, A. M.; Arrio, M.-A.; Cornia, A.; Gatteschi, D.; Sessoli, R. *Nat. Mater.* **2009**, *8*, 194.
- (3) (a) Chandrasekhar, V.; Kingsley, S. *Angew. Chem., Int. Ed.* **2000**, *39*, 2320. (b) Brechin, E. K.; Coxall, R. A.; Parkin, A.; Parsons, S.; Tasker, P. A.; Winpenny, R. E. P. *Angew. Chem., Int. Ed.* **2001**, *40*, 2700. (c) Gopal, K.; Ali, S.; Winpenny, R. E. P. In *Metal Phosphonate Chemistry: From Synthesis to Applications*; Clearfield, A., Demadis, K., Eds.; Royal Society of Chemistry: Cambridge, U.K., 2012; pp 364–419.
- (4) Clearfield, A. *Curr. Opin. Solid State Mater. Sci.* **1996**, *1*, 268.
- (5) Tolis, E. I.; Helliwell, M.; Langley, S. K.; Raftery, J.; Winpenny, R. E. P. *Angew. Chem., Int. Ed.* **2003**, *42*, 3804.

- (6) (a) Langley, S. K.; Helliwell, M.; Raftery, J.; Tolis, E. I.; Winpenny, R. E. P. *Chem. Commun.* **2004**, 142. (b) Langley, S. K.; Helliwell, M.; Sessoli, R.; Rosa, P.; Wernsdorfer, W.; Winpenny, R. E. P. *Chem. Commun.* **2005**, 5029. (c) Langley, S. K.; Helliwell, M.; Sessoli, R.; Teat, S. J.; Winpenny, R. E. P. *Inorg. Chem.* **2008**, *47*, 497. (d) Langley, S. K.; Helliwell, M.; Sessoli, R.; Teat, S. J.; Winpenny, R. E. P. *Dalton Trans.* **2009**, 3102. (e) Langley, S. K.; Helliwell, M.; Teat, S. J.; Winpenny, R. E. P. *Dalton Trans.* **2012**, *41*, 12807.
- (7) (a) Baskar, V.; Shanmugam, M.; Sañudo, E. C.; Shanmugam, M.; Collison, D.; McInnes, E. J. L.; Wei, Q.; Winpenny, R. E. P. *Chem. Commun.* **2007**, 37. (b) Murugavel, R.; Shanmugam, S. *Dalton Trans.* **2008**, 5358. (c) Chandrasekhar, V.; Nagarajan, L.; Clérac, R.; Ghosh, S.; Verma, S. *Inorg. Chem.* **2008**, *47*, 1067.
- (8) Finn, R. C.; Zubieta, J.; Haushalter, R. C. *Prog. Inorg. Chem.* **2003**, *51*, 421.
- (9) (a) Khanra, S.; Kloth, M.; Mansaray, H.; Murny, C. A.; Tuna, F.; Sañudo, E. C.; Helliwell, M.; McInnes, E. J. L.; Winpenny, R. E. P. *Angew. Chem., Int. Ed.* **2007**, *46*, 5568. (b) Khanra, S.; Batchelor, L.; Helliwell, M.; Tuna, F.; McInnes, E. J. L.; Winpenny, R. E. P. *J. Mol. Struct.* **2008**, *890*, 157.
- (10) (a) Shanmugam, M.; Shanmugam, M.; Chastanet, G.; Sessoli, R.; Mallah, T.; Wernsdorfer, W.; Winpenny, R. E. P. *J. Mater. Chem.* **2006**, *16*, 2576. (b) Shanmugam, M.; Chastanet, G.; Mallah, T.; Sessoli, R.; Teat, S. J.; Timco, G. A.; Winpenny, R. E. P. *Chem.—Eur. J.* **2006**, *12*, 8777. (c) Maheswaran, S.; Chastanet, G.; Teat, S. J.; Mallah, T.; Sessoli, R.; Wernsdorfer, W.; Winpenny, R. E. P. *Angew. Chem., Int. Ed.* **2005**, *44*, 5044. (d) Ma, Y.-S.; Song, Y.; Li, Y.-Z.; Zheng, L.-M. *Inorg. Chem.* **2007**, *46*, 5459. (e) Li, J.-T.; Ma, Y.-S.; Li, S.-G.; Cao, D.-K.; Li, Y.-Z.; Song, Y.; Zheng, L.-M. *Dalton Trans.* **2009**, 5029. (f) Konar, S.; Clearfield, A. *Inorg. Chem.* **2008**, *47*, 3489. (g) Wang, M.; Ma, C.; Wen, H.; Chen, C. *Dalton Trans.* **2008**, 4612. (h) Ma, Y.-S.; Yao, H.-C.; Hua, W.-J.; Li, S.-H.; Li, Y.-Z.; Zheng, L.-M. *Inorg. Chim. Acta* **2007**, *360*, 1645. (i) Yao, H.-C.; Li, Y.-Z.; Song, Y.; Ma, Y.-S.; Zheng, L.-M.; Xin, X.-Q. *Inorg. Chem.* **2006**, *45*, 59. (j) Wang, M.; Ma, C.; Yuan, D.; Hu, M.; Chen, C.; Liu, Q. *New J. Chem.* **2007**, *31*, 2103. (k) Wang, M.; Ma, C.-B.; Yuan, D.-Q.; Wang, H.-S.; Chen, C.-N.; Liu, Q.-T. *Inorg. Chem.* **2008**, *47*, 5580. (l) Wang, M.; Ma, C.; Wen, H.; Chen, C. *Dalton Trans.* **2009**, 994.
- (11) (a) Tolis, E. I.; Engelhardt, L. P.; Mason, P. V.; Rajaraman, G.; Kindo, K.; Luban, M.; Matsuo, A.; Nojiri, H.; Raftery, J.; Schroder, C.; Timco, G. A.; Tuna, F.; Wernsdorfer, W.; Winpenny, R. E. P. *Chem.—Eur. J.* **2006**, *12*, 8961. (b) Khanra, S.; Konar, S.; Clearfield, A.; Helliwell, M.; McInnes, E. J. L.; Tolis, E.; Tuna, F.; Winpenny, R. E. P. *Inorg. Chem.* **2009**, *48*, 5338. (c) Khanra, S.; Helliwell, M.; Tuna, F.; McInnes, E. J. L.; Winpenny, R. E. P. *Dalton Trans.* **2009**, 6166. (d) Konar, S.; Bhuvanesh, N.; Clearfield, A. *J. Am. Chem. Soc.* **2006**, *128*, 9604. (e) Konar, S.; Clearfield, A. *Inorg. Chem.* **2008**, *47*, 5573. (f) Yao, H.-C.; Li, Y.-Z.; Zheng, L.-M.; Xin, X.-Q. *Inorg. Chim. Acta* **2005**, *358*, 2523. (g) Yao, H.-C.; Wang, J.-J.; Ma, Y.-S.; Waldmann, O.; Du, W.-X.; Song, Y.; Li, Y.-Z.; Zheng, L.-M.; Decurtins, S.; Xin, X.-Q. *Chem. Commun.* **2006**, 1745. (h) Murugavel, R.; Gogoi, N.; Clérac, R. *Inorg. Chem.* **2009**, *48*, 646.
- (12) (a) Ma, Y.-S.; Song, Y.; Tang, X.-Y.; Yuan, R.-X. *Dalton Trans.* **2010**, 39, 6262. (b) Sheikh, J. A.; Goswami, S.; Adhikary, A.; Konar, S. *Inorg. Chem.* **2013**, *52*, 4147.
- (13) (a) Baskar, V.; Gopal, K.; Helliwell, M.; Tuna, F.; Wernsdorfer, W.; Winpenny, R. E. P. *Dalton Trans.* **2010**, 39, 4747. (b) Wang, M.; Yuan, D.-Q.; Ma, C.-B.; Yuan, M.-J.; Hu, M.-Q.; Li, N.; Chen, H.; Chen, C.-N.; Liua, Q.-T. *Dalton Trans.* **2010**, 39, 7276. (c) Zheng, Y.-Z.; Evangelisti, M.; Winpenny, R. E. P. *Angew. Chem., Int. Ed.* **2011**, *50*, 3692. (d) Zheng, Y.-Z.; Evangelisti, M.; Winpenny, R. E. P. *Chem. Sci.* **2011**, *2*, 99. (e) Zheng, Y.-Z.; Pineda, E. M.; Helliwell, M.; Evangelisti, M.; Winpenny, R. E. P. *Chem.—Eur. J.* **2012**, *18*, 4161. (f) Zheng, Y.-Z.; Evangelisti, M.; Tuna, F.; Winpenny, R. E. P. *J. Am. Chem. Soc.* **2012**, *134*, 1057. (g) Pineda, E. M.; Tuna, F.; Zheng, Y.-Z.; Pritchard, R. G.; Regan, A. C.; Winpenny, R. E. P.; McInnes, E. J. L. *Chem. Commun.* **2013**, 49, 3522. (h) Hooper, T. N.; Schnack, J.; Piligkos, S.; Evangelisti, M.; Brechin, E. K. *Angew. Chem., Int. Ed.* **2012**, *51*, 4633.
- (i) Pineda, E. M.; Tuna, F.; Zheng, Y.-Z.; Winpenny, R. E. P.; McInnes, E. J. L. *Inorg. Chem.* **2013**, *52* (23), 13702–13707.
- (14) (a) Zangana, K. H.; Pineda, E. M.; Schnack, J.; Winpenny, R. E. P. *Dalton Trans.* **2013**, 42, 14045. (b) Zangana, K. H.; Pineda, E. M.; McInnes, E. J. L.; Schnack, J.; Winpenny, R. E. P. *Chem. Commun.* **2014**, accepted for publication.
- (15) Breeze, B. A.; Shanmugam, M.; Tuna, F.; Winpenny, R. E. P. *Chem. Commun.* **2007**, 5185.
- (16) Cosier, J.; Glazer, A. M. *J. Appl. Crystallogr.* **1986**, *19*, 105.
- (17) *SHELX-PC Package*; Bruker Analytical X-ray Systems: Madison, WI, 1998.
- (18) Harris notation describes the binding mode as  $[XY_1Y_2Y_3\dots Y_n]$ , where X is the overall number of metals bound by the whole ligand, and each value of Y refers to the number of metal atoms attached to the different donor atoms. See Coxall, R. A.; Harris, S. G.; Henderson, D. K.; Parsons, S.; Tasker, P. A.; Winpenny, R. E. P. *J. Chem. Soc., Dalton Trans.* **2000**, 2349.

## NOTE ADDED AFTER ASAP PUBLICATION

This paper was published on the Web on January 6, 2014, with incorrect ligands for compounds **1** and **2** throughout the paper. The corrected version was reposted on January 9, 2014.